Available online at www.sciencedirect.com
SCIENCE DIRECT®
European Journal of Medicinal Chemistry 39 (2004) 879–887
EUROPEAN JOURNAL OF MEDICINAL CHEMISTRY
www.elsevier.com/locate/ejmech

Short communication

8-Substituted-9-deazaxanthines as adenosine receptor ligands: design, synthesis and structure-affinity relationships at A_{2B}

Angelo Carotti [a,*], Angela Stefanachi [a], Enrique Raviña [b], Eddy Sotelo [b], Maria Isabel Loza [c], Maria Isabel Cadavid [c], Nuria B. Centeno [d], Orazio Nicolotti [a]

[a] *Dipartimento Farmacochimico,Università di Bari, via Orabona 4, 70125 Bari, Italy*
[b] *Departamento de Quimica Organica, Universidade de Santiago de Compostela, 15782 Santiago de Compostela, Spain*
[c] *Departamento de Farmacologia, Universidade de Santiago de Compostela, 15782 Santiago de Compostela, Spain*
[d] *Grup de Recerca en Informàtica Biomèdica (GRIB), IMIM-UPF, C/Dr. Aiguader 80, 08003 Barcelona, Spain*

Received 12 March 2004; received in revised form 24 June 2004; accepted 7 July 2004

Abstract

A number of 8-substituted-9-deazaxanthine derivatives (1,3-dialkyl-6-substituted-1*H*-pyrrolo[3,2-*d*]pyrimidine-2,4(3*H*,5*H*)-diones) were prepared and tested for their antagonistic activity at the recombinant human adenosine receptors, in particular at the A_{2B} and A_{2A} receptor subtypes. Compounds endowed with micromolar to nanomolar binding affinities, but with poor A_{2B}/A_{2A} selectivity, were obtained. Preliminary quantitative structure–affinity relationships suggested that the binding potency at the A_{2B} receptor is mainly modulated by the electronic and lipophilic properties of the ligands.

Keywords: 1,3-Dialkyl-6-substituted-1*H*-pyrrolo[3,2-*d*]pyrimidine-2,4(3*H*, 5*H*)-diones; Adenosine receptor antagonists; A_{2B} and A_{2A} binding affinities; A_{2A}/A_{2B} selectivity; Quantitative structure–affinity relationships

1. Introduction

Adenosine is a nucleoside that modulates many important physiological functions [1,2] by interacting at four different G-protein coupled receptor subtypes [3] named A_1, A_{2A}, A_{2B} and A_3.[4] A_1 and A_{2A} adenosine receptors (ARs) are stimulated by low adenosine concentrations, whereas higher adenosine levels are required for the activation of A_{2B} and A_3 ARs [5]. A huge number of AR agonists and antagonists have been synthesized so far [6–9] and potent and subtype selective ligands, with high potential in many therapeutic fields, have been discovered. Selective ligands for A_1, A_{2A} and, more recently, A_3 ARs have been made available for biological and pharmacological studies [10–14]. As far as selective A_{2B} receptor ligands are concerned, only few compounds with a relatively low selectivity have been described [15–19]. Selective A_{2B} receptor antagonists are therefore actively pursued since they play a pivotal role in the control of a variety of physiological functions including vascular tone [20], hepatic glucose balance [21], cell growth [22], gene expression [23], mast cell degranulation [24] and intestinal water secretion [25]. More recently, a growing interest for the discovery of selective A_{2B} receptor antagonists stemmed from their potential use as antidiabetic [26] and antiasthmatic agents [27,28].

Xanthine derivatives constitute, along with purine nucleoside analogues and condensed tricyclic nitrogen heterocyclic derivatives [6,7,9,13], one of the most exploited class of AR ligands [17–19,29–31]. In spite of that, xanthines and closely related analogues, appear still appealing since the antiasthmatic activity shown by some xanthine drugs, (i.e. theophylline and enprofylline), has been associated to a slight, but significant, antagonism at the A_{2B} receptor subtypes [32].

As anticipated, many xanthine derivatives have been already investigated as AR antagonists whereas 9-deazaxanthines (9-dAXs) have been only rarely studied [31,33], especially for their antagonist activity at A_{2B} receptors [17]. Therefore, some years ago we begun a systematic study addressing the synthetic accessibility to fully functionalized 9-dAXs and a deep exploration of their biological and pharmacological properties. Herein we report the design,

* Corresponding author. Tel.: +39-080-5442782; fax: +39-080-5442230.
E-mail address: carotti@farmchim.uniba.it (A. Carotti).

0223-5234/$ - see front matter © 2004 Elsevier SAS. All rights reserved.
doi:10.1016/j.ejmech.2004.07.008

Table 1
Chemical structures and affinity binding data of 9-dAX derivatives **1b–19b**

Cp	R	R^1	R^2	p*K*i [a] hA_{2B}	p*K*i [a] hA_{2A}	p*K*i hA_1	p*K*i hA_3
1b	CH_3	C_6H_5	H	6.74	6.32 [b]		
2b	CH_3	4-OH-C_6H_4	H	7.16	6.73		
3b	CH_3	4-NH_2-C_6H_4	H	7.24	6.66		
4b	CH_3	4-NHAc-C_6H_4	H	20%	21%		
5b	CH_3	2-F-C_6H_4	H	0%	13%		
6b	CH_3	2,6-F_2-C_6H_3	H	9%	0%		
7b	CH_3	2-Thienyl	H	7.00	6.09		
8b	CH_3	3-Thienyl	H	7.14	6.58		
9b	CH_3	5-Br-2-thienyl	H	7.41	6.98		
10b	CH_3	2-Furyl	H	6.73	6.42		
11b	CH_3	C_6H_5	CH_3	1% [c]	10% [c]		
12b	CH_3	2-Thienyl	CH_3	3%	16%		
13b	CH_3	2-Furyl	CH_3	12%	18%		
14b	n.C_3H_7	C_6H_5	H	6.64	6.19 [d]	7.47 [d]	7.02
15b	n.C_3H_7	4-NH_2-C_6H_4	H	7.78	6.95		
16b	n.C_3H_7	C_6H_5	OH	6.17	32%	7.60	30%
17b	n.C_3H_7	4-OCH_3-C_6H_4	H	7.59	6.80		
18b	n.C_3H_7	4-OC_3H_7-C_6H_4	H	6.79	5.87		
19b	n.C_3H_7	4-$OCH_2C_6H_5$-C_6H_4	H	6.02	5.60		

[a] Binding affinity is expressed as p*K*i or percent of displacement at 0.1 μmol (1 μmol for compound **16b** at hA_3). *K*i and percent of displacement had a SEM <10%. For compound **16b**, the EC_{50} at hA_{2B} is reported.
[b] Lit. p*K*i (rat brain, rA_2), 6.29 [33].
[c] Lit. p*K*i value (rat brain) 4.40 and 4.95 at rA_2 and rA_1, respectively, [33].
[d] Lit. p*K*i values (rat brain) 6.35 and 7.88 at rA_2 and rA_1, respectively, [33].

synthesis and AR binding affinities, mainly at the A_{2B} and A_{2A} subtypes, of a series of 1,3-dialkyl-(7,)8-(di)substituted-9-deazaxanthines, whose chemical structures are reported in Table 1. Our main goals were the discovery of new molecular entities endowed with high affinity and, possibly, good selectivity towards the A_{2B} receptor subtype and the development of preliminary structure–affinity relationships, at A_{2B} receptors, and structure–selectivity (A_{2B}/A_{2A}) relationships able to suggest further structural modifications of the 9-dAX skeleton to improve both potency and selectivity.

2. Chemistry

Compounds **1b**, **2b**, **4b–10b**, **14b**, **18b** and **19b** were prepared starting from the corresponding 1,3-dialkyl-6-methyl-5-nitrouracyls according the synthetic pathway outlined in Scheme 1 [33].

The amino derivatives **3b** and **15b** were obtained trough the basic hydrolysis of the corresponding 1,3-dimethyl [**4b**] and 1,3-dipropyl [35] acetamido derivatives, respectively, whereas the N_7-methyl derivatives **11b–13b** were synthesi-

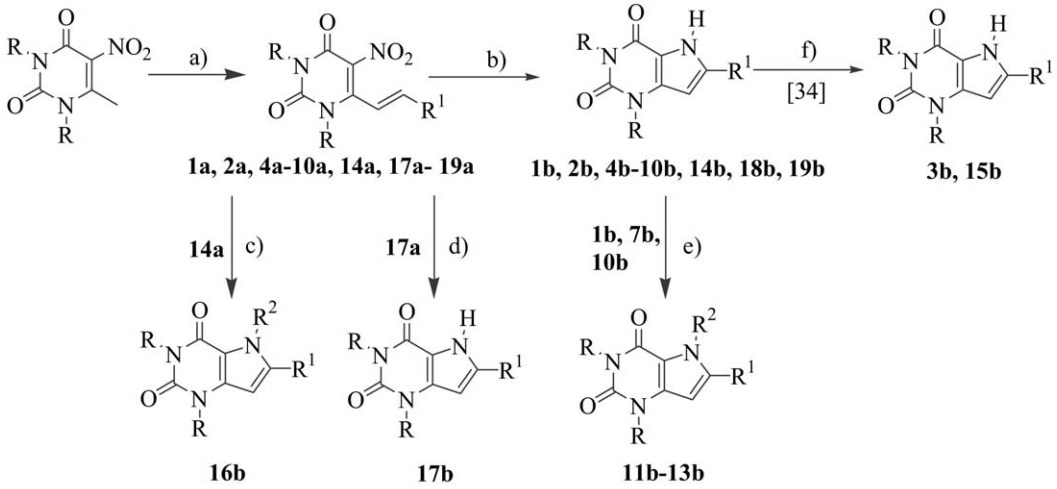

a) R^1CHO, piperidine, EtOH, reflux 8h, 45-75% yields b) $(EtO)_3P$, reflux 7h, 10-15% yields,
c) $SnCl_2$, DMF, r.t., 5 min, 95% yields; d) $SnCl_2$, DMF, reflux 2 h, 95% yields;
e) CH_3I, K_2CO_3, DMF, 0°C, 65-75% yields; f) NaOH, EtOH reflux.

Scheme 1. Synthetic pathway to 9-dAX derivatives.

zed by alkylation of the corresponding N_7H derivatives **1b**, **7b** and **10b** with methyl iodide and K_2CO_3 in DMF. Finally, the *p*-OCH_3 phenyl derivative **17b** the N_7–OH derivative **16b** were prepared from the corresponding 5-nitro-6-styryluracyl precursor through an efficient reductive cyclization reaction, recently reported by some of us [35].

3. Pharmacology

Compounds were tested for their ability to displace [^{3}H]-DPCPX, [^{3}H]-ZM241385, [^{3}H]-DPCPX and [^{3}H]-NECA from cloned human A_1, A_{2A}, A_{2B} and A_3 ARs, respectively. Assays were carried out by coincubation of compounds, in at least six different concentrations, with the appropriate radioactive ligand. Adenylyl cyclase functional assay was performed to determine the intrinsic activity of compound **16b** at A_{2B} receptors.

4. Results and discussion

Preliminarily, the 9-dAX ring system was compared to that of xanthines, to detect some physicochemical differences, especially in terms of electronic characteristics, ability to make hydrogen bonds (HBs), water solubility and partition in apolar/polar immiscible solvents. A straightforward comparison of the molecular electrostatic potentials (MEPs) [36,37], performed by means of the MIPSIM software [38], of two model compounds, that are 8-methyltheophylline and its corresponding 9-deaza analogue, depicted in Fig. 1, indicates the lack of the deepest MEP minimum of 8-methyltheophylline in the corresponding 9-deaza analogue, a fact that may strongly influence the ability of making HB and/or participating to other electrostatic (polar) interactions.

As for the physicochemical properties relevant to the ADME profile, both a higher water solubility and octanol/water partition coefficient can be assessed by ACD [39] and c-LOGP [40] software, respectively, for 9-dAXs compared with the corresponding xanthine analogues.

The above observations were in full agreement with the quite diverse biological profiles, structure–activity and structure–selectivity relationships observed for the two classes of ligands [41].

As far as the AR affinity of 9-dAXs is concerned, an examination of the data in Table 1 revealed that relatively potent, but poorly selective, A_{2B} receptor ligands were obtained.

Interestingly, affinities at A_{2B} receptor subtype were found to be generally higher than those observed at A_{2A} receptor, with the most selective compounds **18b**, **7b** and **15b** having a *K*i (A_{2A})/*K*i (A_{2B}) ratio of 8.3, 8.1 and 6.8, respectively.

Isosteric substitution of the 8-phenyl ring of the 1,3-dimethyl-9-dAXs generally improved the activity; the most active isoster, i.e. the 3-thienyl derivative **8b**, had a p*K*i = 7.14. The introduction of a 5-bromo substituent in the thienyl ring of compound **7b**, yielded derivative **9b** that displayed a higher affinity at both A_{2A} and A_{2B} receptors. Notably, the less lipophilic 2-furyl derivative **10b**, showed at the A_{2B} receptor subtype an affinity lower than the thienyl isosters **7b** and **8b**. Substitution at the *para* position of the 8-phenyl ring with hydrophilic and/or electron-donor groups afforded a significant increase of activity (see cps **2b**, **3b** and **17b**) whereas a hydrophilic substituent with a low electronic effect induced a drastic decrease of affinity (i.e. cp **4b**). An even more dramatic drop of affinity was observed in the *ortho*-substituted fluoro derivatives **5b** and **6b**. Most likely, a strong intramolecular HB between the H at N_7 and the *ortho*-fluoro substituent of the phenyl at C_8 might preclude, or strongly limit, the formation of a favourable HB (donor) interaction of the N_7H with an acceptor group on the receptorial counter part. This hypothesis is supported by the lack of activity observed in N_7-methylated derivatives **11b–13b**. Interestingly, the N_7–OH derivative **16b**, which may be able

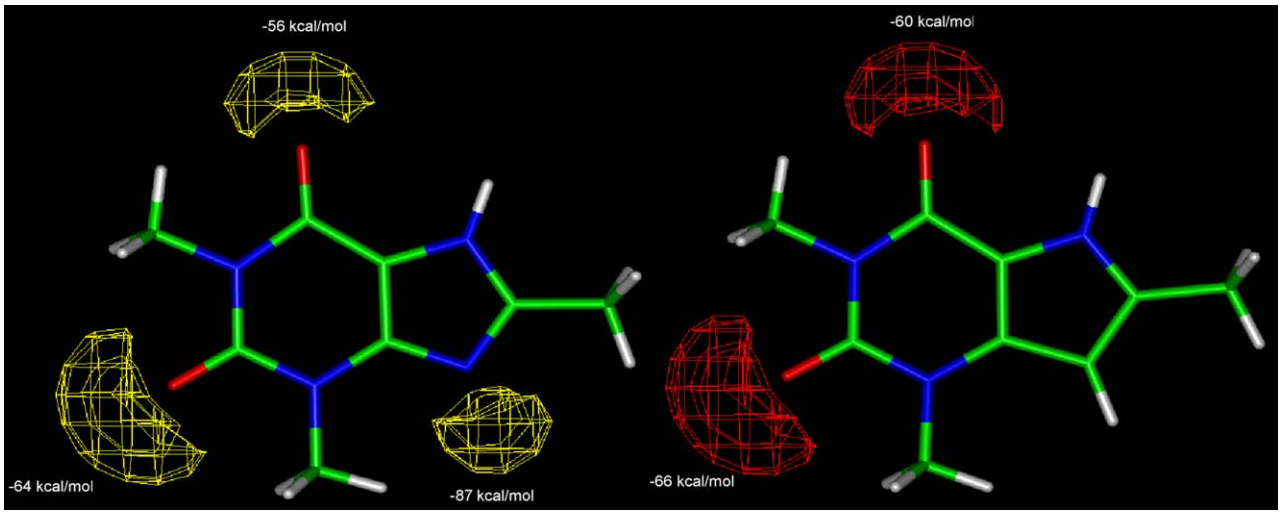

Fig. 1. MEP[36] minimum regions of 8-methyltheophylline (yellow contours, left-hand side) and of its 9-deaza analogue (red contours, right-hand side). The values of the local deepest minima are indicated in kcal/mol.

to engage an HB (donor) interaction, recovered some affinity at A_{2B} and, at least in part, at A_{2A} AR subtypes.

It is worth noting that the N_7–OH derivative **16b** is a potent and highly selective ligand at the A_1 receptor. Finally, a further structural variation was explored by replacing the methyl groups at positions 1,3 of **1b** and **3b** with *n*-propyl groups. While for the former, as already reported [33], a little change of activity was observed (i.e. cp **14b**), a strong increase of activity was measured for its *para*-NH_2-substituted congener **15b**. Within the examined series of compounds, the anilino derivative **15b** proved to be the most active ligand at the A_{2B} receptor subtype.

To gain, at a quantitative level, further insights on the most important physicochemical properties modulating the binding affinity at A_{2B} receptor, biological data in Table 1 were subjected to a QSAR study by means of a multivariate linear regression analysis [42] (Hansch-type approach) [43] with cross validation. Unfortunately, our dataset was too small for a secure application of 3D QSAR methods.

Classical substituent (molecular) descriptors assessing electronic (σ, E_{HOMO}, E_{LUMO}) steric (MR, van der Waals volumes, Verloop (L, B_1, B_5)) and lipophilic parameters (LOGP, π were taken from standard compilations [44] or calculated by means of known software such as the c-LOGP [40]. The ones used for the development of regression equation shown below are listed in Table 2.

Compound **16b** was not considered in the QSAR analysis as it presented unique structural elements compared to the congeneric series of compounds listed in Table 1. Moreover, for this compound only the intrinsic activity was measured.

Preliminary one- and two-term models derived from σ and c-LOGP, the latter tested both as a linear and as a quadratic term, resulted in very poor statistics ($r^2 < 0.30$). These disappointing findings can be to some extent related to the presence of some peculiar structural patterns that the model was still unable to quantify. And in fact, a close look at the structural features of the molecules in the dataset easily led to the identification of two particular groups of compounds: the first is constituted by two *ortho*-fluoro substituted derivatives (**5b** and **6b**) at the 8-phenyl ring and the second by three N_7–CH_3 derivatives (**11b–13b**). As expected, the removal of these two groups of molecules consistently increased the model fitting capability ($r^2 = 0.653$). It should be added that such a model came from only 13 compounds whose activity was spread in a very narrow range (6.20–7.78). The need to recover most of the structural and biological information contained in our dataset prompted us to make use of nominal variables to explain the impact on QSAR of the *ortho*-fluoro and of N_7–CH_3 substituted derivatives. Our efforts was awarded by the following equation:

$$p\,Ki = 5.310\,(\pm 0.472) - 0.230\,(\pm 0.091)\,\sigma + 1.200\,(\pm 0.310)\ \text{cLOGP} - 0.181\,(\pm 0.043)\ \text{cLOGP}^2 - 1.937\,(\pm 0.276)\ I_1 - 2.097\,(\pm 0.211)\ I_2$$

$$n = 18,\ r^2 = 0.933,\ s = 0.308,\ q^2 = 0.851$$

where *n*, r^2, *s* and q^2 are statistical parameters indicating the numbers of data points, the squared correlation coefficient, the standard deviation and the squared cross-validation correlation coefficient (based on the leave-one-out procedure [45]), respectively. Figures in parentheses represent the standard errors of the regression coefficients.

It must be underlined that for ligands with low binding affinity at A_{2B} receptor (up to 12% displacement at 0.1 μM), that are compounds **5b**, **6b**, **11b**, **12b** and **13b**, a censored (truncated) p*K*i value, arbitrarily set to 5.00, was used for the

Table 2
Affinity binding data and descriptors used for the derivation of QSAR equation

Cp	p*K*i (obs)	p*K*i (calc) [a]	σ [b]	c-LOGP	I_1 [c]	I_2 [c]
1b	6.74	7.16	–0.01	2.35	0	0
2b	7.16	7.06	–0.10	1.69	0	0
3b	7.24	6.92	–0.21	1.13	0	0
4b	6.20	6.64	–0.01	1.37	0	0
5b	5.00	5.07	0.08	2.51	1	0
6b	5.00	4.93	0.16	2.66	1	0
7b	7.00	6.98	0.05	2.22	0	0
8b	7.14	7.05	–0.02	2.01	0	0
9b	7.41	6.90	0.16	2.81	0	0
10b	6.73	6.81	0.02	1.74	0	0
11b	5.00[d]	5.16	–0.01	2.64	0	1
12b	5.00[d]	4.98	0.05	2.50	0	1
13b	5.00[d]	4.87	0.02	2.03	0	1
14b	6.64	7.10	–0.01	4.47	0	0
15b	7.78	7.80	–0.21	3.24	0	0
17b	7.59	7.29	–0.08	4.40	0	0
18b	6.79	6.68	–0.08	5.46	0	0
19b	6.02	6.05	–0.08	6.17	0	0

[a] Values calculated from our QSAR equation.
[b] Hammett sigma constants refer to the R^1 substituent.
[c] Indicator variables (see text for definition).
[d] Censored (truncated) values.

derivation of QSAR. Moreover, in the development of the QSAR models, the σ values reported in Table 2 were multiplied by 10 to obtain a new set of values, more or less equiscalar with those of c-LOGP, I_1 and I_2.

In the above equation, σ refers to the Hammett constant of the R^1 substituents whereas I_1 and I_2 are indicator variables that take into account the presence/absence of *ortho*-fluoro substituents at the 8-phenyl ring and of N_7–CH_3 groups, respectively. Briefly, I_1 is set to 1 for compounds **5b** and **6b** and to 0 for all the remaining ones while I_2 is set to 1 for compounds **11b–13b** with all the others being set to 0. As repeatedly observed in QSAR modelling, [43] a linear relationship with lipophilicity can hold only up to a certain maximum LOGP (or π) value (formally termed $LOGP_0$ or π_0) beyond which a decrease of activity can be observed, and this is the case also for our equation: the compound with the highest activity (**15b**, p*K*i = 7.78) showed a c-LOGP = 3.24, a value close to the theoretical $LOGP_0$ (nearly 3.30). Moreover, the high activity of **15b** is thought to derive also by its strong electron-donor properties. A drastic lowering of activity was observed for ligands with c-LOGP >>3.24 such as compounds **14b**, **18b** and **19b**. A parabolic profile (data not shown) resulted by plotting c-LOGP vs. p*K*i being the three compounds just mentioned located on the bottom descending part of the curve.

A further way to prove the goodness of the applicability domain of the above equation is the analysis of the leverages [46] which represent the distance of a given compound from the centre of the experiments. The ability of making a prediction is smoothly reduced when the leverage value moves away from such a centre. It is generally accepted that a warning leverage results when the value $3p/n$ is overcome. In this ratio, p represents the number of parameters of a model and n the number of objects, respectively. Very satisfying all the leverages values calculated for our equation were lower than $3p/n$.

In order to confirm that the model shown in the equation did not represent a spurious regression, a randomisation test was conducted. In doing that, the dependent variables of Table 2 were scrambled 30 times and a linear regression analysis was performed for each resulting data sequence. The best model, among the 30 ones obtained, showed statistics ($r^2 = 0.667$ and $q^2 = 0.324$) much poorer than those observed in the unscrambled equation. This result made us more confident on the statistical reliability of our QSAR model.

Within the limit of the low number of data points and the narrow physicochemical space explored, our QSAR equation suggested that the binding affinity at A_{2B} receptors increases as the electron-donor character of substituents at position 8 and the overall molecular lipophilicity increase, but only up to the optimal c-LOGP values which is close to 3.30. The high and negative regression coefficients associated with the I_1 and I_2 indicator variables, quantified well the dramatic drop of affinity caused by both the *ortho*-phenyl substitution and the N_7-methylation.

5. Conclusion

The results reported in the present paper demonstrated that 8-aryl(heteroaryl)substituted-9-deazaxanthines might be considered a promising class of compounds to develop potent and, hopefully, selective ligands at the ARs, in particular at the A_{2B} receptor subtype. The most salient features of the SAFIR and, to a lesser extent, SSR (structure–selectivity relationship) coming from the present study have been used as a starting point for the design of new selective A_{2B} receptor ligands. The outcome of these ongoing studies will be reported in due course in forthcoming papers.

6. Experimental protocols

6.1. Chemistry

General Information. All reactions were carried out under an argon atmosphere. Reagent grade solvents were dried according to standard techniques. Magnesium sulphate was used as a drying agent for water containing organic phases. Thin-layer chromatography (TLC) was performed by using aluminium sheets precoated with silica gel 60 F_{254} (0.2 mm) E. Merck. Chromatographic spots were visualised by UV light or Hannessian reagent. Purification of crude compounds and separation of reaction mixtures were carried out by column chromatography on silica gel 60 (0.040–0.063 mm, E. Merck) using appropriate eluents. Melting points (uncorrected) were determined in a Gallenkamp melting point apparatus. Chemical shifts (δ) are reported in parts per million (ppm) relative to the solvent central peak . Coupling constant (J values) are given in Hertz (Hz). ^{1}HNMR spectra were recorded at 300 MHz on a Bruker AMX-300 spectrometer. Low resolution mass spectra were determined in a quadrupolar Hewlett-Packard 5988 mass spectrometer by electronic impact (MS-EI). The molecular weights and the fragmentation patterns from the MS spectra (not reported) were in full agreement with the proposed chemical structures. The purity of intermediates **1a–10a**, **14a**, **18a** was checked by HPLC (Waters 1525 Binary HPLC pump, Phenomenex C_{18}). Elemental analyses were performed on a Carlo Erba C, H, N analyser. All final products had satisfactory C, H, N analyses (within ±0.40 of theoretical values). The syntheses of 8-aryl-9-deazaxanthines **1b** [33], **14b** [33] **16b** [35] and **17b** [35] have been already described.

6.1.1. General procedure for the condensation between aromatic aldehydes and 1,3-dialkyl-6-methyl-5-nitrouracils

A solution of the 6-methyl-5-nitro-pyrimidine-2,4-dione (30 mmol), the appropriate aldehyde (30 mmol) and piperidine (45 mmol) in dry dioxane was refluxed for 5–8 h. The solution was concentrated under vacuum and the residue was treated with ethanol under stirring until a precipitate was formed. The solid was collected by filtration and dried under vacuum to yield the expected 6-alkenyl-substituted uracyl derivative.

*6.1.1.1. 6-[(E)-2-(4-hydroxyphenyl)-vinyl]-1,3-dimethyl-5-nitro-pyrimidine-2,4(1H,3H)-dione [**2a**].* Yield 35% ^{1}HNMR (acetone d_6): 7.50 (d, *J* = 14.9 Hz, 1H), 6.90 (m, 5H), 3.50 (s, 3H), 3.45 (s, 3H).

6.1.1.2. N-*{4[(E)-2-(1,3-dimethyl-5-nitro-2,6-dioxo-1,2,3,6-tetrahydropyrimidin-4-yl)-vinyl]-phenyl}-acetamide [**4a**].* Yield 38% ^{1}HNMR (DMSO d_6): 7.58 (m, 4H), 6.83 (m, 2H), 3.28 (s, 3H), 3.17 (s, 3H), 2.17 (s, 3H).

*6.1.1.3. 6-[(E)-2-(2-fluorophenyl)-vinyl]-1,3-dimethyl-5-nitro-pyrimidine-2,4(1H,3H)-dione [**5a**].* Yield 42% ^{1}HNMR ($CDCl_3$): 7.31 (d, *J* = 14.9 Hz, 1H), 7.40 (m, 4H), 6.95 (d, *J* = 14.9 Hz, 1H), 3.44 (s, 3H), 3.36 (s, 3H).

*6.1.1.4. 6-[(E)-2-(2,6-difluorophenyl)-vinyl]-1,3-dimethyl-5-nitro-pyrimidine-2,4(1H,3H)-dione [**6a**].* Yield 22% ^{1}HNMR ($CDCl_3$): 7.29 (m, 1H), 7.18 (d, 1H, *J* = 18.0 Hz), 7.05 (d, 1H, *J* = 18.0 Hz), 6.79 (m, 2H), 3.51 (s, 3H), 3.43 (s, 3H).

*6.1.1.5. 1,3-dimethyl-5-nitro-6-[(E)-2-(thien-2-yl)-vinyl]-pyrimidine-2,4(1H,3H)-dione [**7a**].* Yield 53% ^{1}HNMR ($CDCl_3$): 7.49 (m, 1H), 7.30 (m, 1H), 7.26 (d, 1H, *J* = 16.4 Hz), 7.11 (m, 1H), 6.47 (d, 1H, *J* = 16.4 Hz), 3.56 (s, 3H) 3.47 (s, 3H).

*6.1.1.6. 1,3-dimethyl-5nitro-6-[(E)-2-(thien-3-yl)-vinyl]-pyrimidine-2,4(1H,3H)-dione [**8a**].* Yield 35% ^{1}HNMR ($CDCl_3$): 7.92 (m, 1H), 7.67 (m, 2H), 7.10 (m, 2H), 3.42 (s, 3H), 3.36 (s, 3H).

*6.1.1.7. 1,3-dimethyl-5-nitro-6-[(E)-2-(5-bromo-thien-2-yl)-vinyl]-pyrimidine-2,4(1H,3H)-dione [**9a**].* Yield 47% ^{1}HNMR ($CDCl_3$): 7.11 (d, 1H, *J* = 16.5 Hz), 7.00 (m, 2H), 6.30 (d, 1H, *J* = 16.5 Hz), 3.44 (s, 3H) 3.34 (s, 3H).

*6.1.1.8. 6-[(E)-2-(fur-2-yl)-vinyl]-1,3-dimethyl-5-nitro-pyrimidine-2,4(1H,3H)-dione [**10a**].* Yield 39% ^{1}HNMR ($CDCl_3$): 7.68 (m, 1H), 7.62 (m, 4H), 3.56 (s, 3H) 3.47 (s, 3H).

*6.1.1.9. 6-[(E)-2(4-propoxyphenyl)-vinyl]-1,3-dipropyl-5-nitro-pyrimidine-2,4(1H,3H)-dione [**18a**].* Yield 41% ^{1}HNMR ($CDCl_3$): 7.38 (d, 2H, *J* = 8.8 Hz), 6.99 (d, 1H, *J* = 16.5 Hz), 6.91 (d, 2H, *J* = 8.8 Hz), 6.45 (d, 1H, *J* = 16.5 Hz), 3.95 (m, 6H), 1.77 (m, 6H) 1.00 (m, 9H).

*6.1.1.10. 6-[(E)-2(4-benzyloxyphenyl)-vinyl]-1,3-dipropyl-5-nitro-pyrimidine-2,4(1H,3H)-dione [**19a**].* Yield 41% ^{1}HNMR ($CDCl_3$): 7.34 (m, 7H), 6.99 (m, 3H), 6.45 (d, 1H, *J* = 16.5 Hz), 5.10 (s, 2H) 3.90 (m, 4H), 1.71 (m, 4H) 0.96 (m, 6H).

*6.1.2. General procedure for the reductive cyclization reaction of 1,3-dialkyl-5-nitro-6-alkenyl-substituted uracyls to 1-*H*-pyrrolo-[3,2-*d*]-pyrimidin-2,4-dione derivatives*

A solution of the appropriate 1,3-dialkyl-5-nitro-6-alkenyl-substituted uracyl intermediate (3.00 mmol) in triethyl phosphite (5 ml) was refluxed for 7 h. The solid formed upon cooling was collected, washed with ethyl ether and crystallized from a water/MeOH mixture to yield the 9-deazaxanthine derivatives listed below:

*6.1.2.1. 6-(4-hydroxyphenyl)-1,3-dimethyl-1*H*-pyrrolo-[3,2-*d*]-pyrimidine-2,4(3*H*,5*H*)-dione [**2b**].* Yield: 15%; m.p.>250 °C ^{1}HNMR (DMSO d_6): 12.1 (s, 1H), 9.70 (s, 1H), 7.72 (d, 2H, *J* = 8.6 Hz), 6.79 (d, 2H, *J* = 8.6 Hz), 6.53 (s, 1H), 3.40 (s, 3H), 3.24 (s, 3H).

6.1.2.2. N-*[4-(1,3-dimethyl-2,4-dioxo-2,3,4,5-tetrahydro-1*H*-pyrrolo[3,2-*d*]-pyrmidin-6-yl)-phenyl]-acetamide [**4b**].* Yield: 25%; m.p.>250 °C ^{1}HNMR (DMSO d_6): 12.27 (s, 1H), 10.05 (s, 1H), 7.83 (d, 2H, *J* = 8.7 Hz), 7.62 (d, 2H, *J* = 8.7 Hz), 6.63 (s, 1H), 3.40 (s, 3H), 3.24 (s, 3H), 2.43 (s, 3H).

*6.1.2.3. 6-(2-Fluorophenyl)-1,3-dimethyl-1*H*-pyrrolo-[3,2-*d*]-pyrimidine-2,4(3*H*,5*H*)-dione [**5b**].* Yield 37% m.p.> 250 °C ^{1}HNMR (DMSO d_6): 12.42 (s, 1H), 7.94 (m, 1H), 7.34 (m, 3H), 6.56 (s, 1H), 3.42 (s, 3H), 3.26 (s, 3H).

*6.1.2.4. 6-(2,6-Difluorophenyl)-1,3-dimethyl-1*H*-pyrrolo-[3,2-*d*]-pyrimidine-2,4(3*H*,5*H*)-dione [**6b**].* Yield 12% m.p.>250 °C ^{1}HNMR (DMSO d_6): 12.40 (s, 1H), 7.51 (m, 1H), 7.27 (m, 2H), 6.44 (s, 1H), 3.40 (s, 3H), 3.25 (s, 3H).

*6.1.2.5. 1,3-Dimethyl-6-(thien-2-yl)-1*H*-pyrrolo-[3,2-*d*]-pyrimidine-2,4(3*H*,5*H*)-dione [**7b**].* Yield 22% m.p.>250 °C ^{1}HNMR (DMSO d_6) 12.50 (s, 1H), 7.68 (dd, 1H, *J* = 3.7, 1.0 Hz), 7.56 (dd, 1H, *J* = 5.0, 1.0 Hz), 7.12 (m, 1H), 6.45 (s, 1H), 3.39 (s, 3H), 3.24 (s, 3H).

*6.1.2.6. 1,3-Dimethyl-6-(thien-3-yl)-1*H*-pyrrolo-[3,2-*d*]-pyrimidine-2,4(3*H*,5*H*)-dione [**8b**].* Yield 20% m.p.>250 °C ^{1}HNMR (DMSO d_6): 12.33 (s, 1H), 8.06 (dd, 1H, *J* = 2.4, 1.6 Hz), 7.65 (m, 2H), 6.60 (s, 1H), 3.40 (s, 3H), 3.25 (s, 3H).

*6.1.2.7. 1,3-Dimethyl-6-(5-bromo-thien-2-yl)-1*H*-pyrrolo-[3,2-*d*]-pyrimidine-2,4(3*H*,5*H*)-dione [**9b**].* Yield 17% m.p.>250 °C ^{1}HNMR (DMSO d_6): 12.57 (s, 1H), 7.43 (d, 1H, *J* = 3.9 Hz), 7.20 (d, 1H, *J* = 3.9 Hz), 6.49 (s, 1H), 3.38 (s, 3H), 3.24 (s, 3H).

*6.1.2.8. 6-(Fur-2-yl)-1,3-dimethyl-1*H*-pyrrolo-[3,2-*d*]-pyrimidine-2,4(3*H*,5*H*)-dione [**10b**].* Yield 14% m.p.>250 °C ^{1}HNMR (DMSO d_6):12.50 (s, 1H), 7.76 (d, 1H, *J* = 1.3), 7.06 (d, 1H, *J* = 3.2 Hz), 6.61 (dd, 1H *J* = 3.2, 1.3 Hz), 6.46 (s, 1H), 3.40 (s, 3H), 3.24 (s, 3H).

*6.1.2.9. 6-(4-Propoxyphenyl)-1,3-dipropyl-1*H*-pyrrolo-[3,2-*d*]-pyrimidine-2,4(3*H*,5*H*)-diones [**18b**].* Yield 33%. m.p. >179–180 °C. ^{1}HNMR (DMSO d_6): 12.18 (s, 1H), 7.83 (d, 2H, *J* = 8.7 Hz), 6.96 (d, 2H, *J* = 8.7 Hz), 6.62 (s, 1H), 3.91 (m, 6H), 1.62 (m, 6H), 0.81 (m, 9H).

*6.1.2.10. 6-(4-Benzyloxyphenyl)-1,3-dipropyl-1*H*-pyrrolo-[3,2-*d*]-pyrimidine-2,4(3*H*,5*H*)-diones **[19b]**.* Yield 37%. m.p. >198–199 °C. ^{1}HNMR (DMSO d_6): 12.18 (s, 1H), 7.84 (d, 2H, *J* = 8.8 Hz), 7.38 (m, 5H) 7.06 (d, 2H, *J* = 8.8 Hz), 6.63 (s, 1H), 5.13 (s, 2H) 3.84 (m, 4H), 1.61 (m, 4H), 0.87(m, 6H).

*6.1.3. Synthesis of 6-(4-aminophenyl)-1,3-dialkyl-1*H*-pyrrolo-[3,2-*d*]-pyrimidine-2,4(3*H*,5*H*)-diones **[3b]** and **[15b]***

N-[4-(1,3-dimethyl-2,4-dioxo-2,3,4,5-tetrahydro-1*H*-pyrrolo[3,2-*d*]-pyrimidin-6-yl)-phenyl]-acetamide [**4b**] or *N*-[4-(1,3-dipropyl-2,4-dioxo-2,3,4,5-tetrahydro-1*H*-pyrrolo[3,2-*d*]-pirimidin-6-yl)-phenyl]-acetamide [35] (0.160 mmol) was dissolved in a mixture of 10% aqueous solution of NaOH (1 ml) and EtOH (1 ml), followed by 2 h refluxing. The solid precipitate was filtered, washed with EtOH and crystallized from a water/MeOH mixture.

*6.1.3.1. 6-(4-Aminophenyl)-1,3-dimethyl-1*H*-pyrrolo-[3,2-*d*]-pyrimidine-2,4(3*H*,5*H*)-dione **[3b]**.* Yield 45%. m.p. >250 °C. ^{1}HNMR (DMSO d_6): 11.96 (s, 1H), 7.59 (d, 2H, *J* = 8.6 Hz), 6.59 (d, 2H, *J* = 8.6 Hz), 6.43 (s, 1H), 5.45 (br, 2H), 3.40 (s, 3H) and 3.25 (s, 3H).

*6.1.3.2. 6-(4-Aminophenyl)-1,3-dipropyl-1*H*-pyrrolo-[3,2-*d*]-pyrimidine-2,4(3*H*,5*H*)-dione **[15b]**.* Yield 35%. m.p. >250 °C. ^{1}HNMR (DMSO d_6): 11.89 (s, 1H), 7.57 (d, 2H, *J* = 8.3 Hz), 6.56 (d, 2H, *J* = 8.3 Hz), 6.43 (s, 1H), 5.38 (br, 2H), 3.81 (m, 4H), 1.60 (m, 4H), 0.87 (m, 6H).

*6.1.4. Synthesis of 6-(aryl or heteroaryl)-1,3,5-trimethyl-1*H*-pyrrolo-[3,2-*d*]-pyrimidine-2,4(3*H*,5*H*)-diones **[11b]**, **[12b]** and **[13b]***

One mmol of the appropriate 9-deazaxanthine was dissolved in DMF (3 ml). K_2CO_3 (2.76 g, 20 mmol) and MeI (0.62 ml, 10 mmol) were added, followed by heating at 50 °C for 4 h. Upon the addition of water (10 ml) the desired compound, precipitated from the solution, was filtered and recrystallized from EtOH.

*6.1.4.1. 1,3,5-Trimethyl-6-phenyl-1*H*-pyrrolo-[3,2-*d*]-pyrimidine-2,4(3*H*,5*H*)-dione **[11b]**.* Yield 93%. m.p. 190–191 °C. ^{1}HNMR ($CDCl_3$): 7.44 (m, 5H), 5.95 (s, 1H), 3.95 (s, 3H), 3.47 (s, 3H) and 3.41 (s, 3H).

*6.1.4.2. 1,3,5-Trimethyl-6-(thien-2-yl)-1*H*-pyrrolo-[3,2-*d*]-pyrimidine-2,4(3*H*,5*H*)-dione **[12b]**.* Yield 95%. m.p. 187–188 °C. ^{1}HNMR ($CDCl_3$): 7.42 (dd, 1H, *J* = 4.9, 1.0 Hz), 7.22 (m, 1H), 7.13 (m, 1H), 6.01 (s, 1H), 4.08 (s, 3H), 3.45 (s, 3H) and 3.41 (s, 3H).

*6.1.4.3. 1,3,5-Trimetyl-6-(fur-2-yl)-1*H*-pyrrolo-[3,2-*d*]-pyrimidine-2,4(3*H*,5*H*)-dione **[13b]**.* Yield 95%. m.p. 187–188 °C. ^{1}HNMR ($CDCl_3$): 7.53 (d, *J* = 1.5 Hz, 1H), 6.63 (d, *J* = 3.4 Hz, 1H), 6.50 (m, 1H), 6.17 (s, 1H), 4.17 (s, 3H), 3.46 (s, 3H) and 3.40 (s, 3H).

6.2. Pharmacology

6.2.1. Radioligand binding assays

Radioligand binding competition assays were performed in vitro using A_1, A_{2A}, A_{2B} and A_3 human receptors expressed in transfected CHO (A_1), HeLa (A_{2A} and A_3) and HEK-293 (A_{2B}) cells. The experimental conditions used are given in details in Table 3.

In each instance aliquots of membranes (15 μg for A_1, 10 μg for A_{2A}, 18 μg for A_{2B} and 90 μg for A_3) in buffer A (see Table 3) were incubated for the specified period of time at 25 °C with the radioligand (2–35 nM) and six different concentrations (ranging from 1 nM to 5 μM) of the test molecule, or standard, in a final volume of 200 μl. The binding reaction was stopped by rapid filtration in a multiscreen manifold system (Millipore Iberica, Madrid, Spain). Unbound radioligand was removed by washing 4× with 250 μl ice-cold buffer B for A_1 and A_{2A} receptors and 6× 250 μl ice-cold buffer B for A_{2B} and A_3 receptors. Non-specific binding was determined using a 50–400 μM NECA soln for A_{2A} and A_{2B} receptors and 10–100 μM R-PIA soln for A_1 and A_3. Radioactivity retained on filters was determined by liquid scintillation counting using Universol (ICN Biochemicals, Inc.). The binding affinities were determined using [^{3}H]-DPCPX as the radioligand for A_1 and A_{2B}, [^{3}H]-ZM241385 for A_{2A} and [^{3}H]-NECA for A_3. The inhibition constant (*K*i) was calculated from IC_{50} by the Cheng and Prusoff [47] equation $Ki = IC_{50}/(1+(C/K_D))$, where IC_{50} is the concentration of compound that displaces the binding of radioligand by 50%, *C* is the free concentration of radioligand and K_D is its apparent dissociation constant.

Table 3
Experimental conditions used for radioligand binding assays on recombinant human A_1, A_{2A}, A_{2B}, and A_3 receptors

	hA_1	hA_{2A}	hA_{2B}	hA_3
Buffer A	20 mM Hepes, 100 mM NaCl, 10 mM $MgCl_2$, 2 units/ml adenosine deaminase (pH 7.4)	50 mM Tris–HCl, 1 mM EDTA, 10 mM $MgCl_2$, 2 units/ml adenosine deaminase (pH 7.4)	50 mM Tris–HCl, 1 mM EDTA, 10 mM $MgCl_2$, 0.1 mM benzamidine, 2 units/ml adenosine deaminase (pH 6.5)	50 mM Tris–HCl, 1 mM EDTA, 5 mM $MgCl_2$, 2 units/ml adenosine deaminase (pH 7.4)
Buffer B	20 mM Hepes, 100 mM NaCl, 10 mM $MgCl_2$, (pH 7.4)	50 mM Tris–HCl, 1 mM EDTA, 10 mM $MgCl_2$ (pH 7.4)	50 mM Tris–HCl (pH 6.5)	50 mM Tris–HCl (pH 7.4)
Plate	GF/C	GF/C	GF/B	GF/B
Radioligand	[^{3}H]-DPCPX 2 nM	[^{3}H]-ZM241385 3 nM	[^{3}H]-DPCPX 35 nM	[^{3}H]-NECA 30 nM
Non-specific binding	10 μM (R)-PIA	50 μM NECA	400 μM NECA	100 μM (R)-PIA
Incubation	25 °C/60 min	25 °C/30 min	25 °C/30 min	25 °C/180 min

6.2.2. cAMP assay

The assay was performed on human A_{2B} receptors transfected in CHO cells by the method described by Salomon [48]. Briefly cells were seeded in 12-well culture plates and incubated at 37 °C in an atmosphere of 5% CO_2 in Dulbecco's Modified Eagle's Medium Nutrient Mixture F-12 (DMEM F-12), containing 10% foetal calf serum (FCS) and 1% L-glutamine. This medium was replaced 24 h before the assays by a medium containing dialyzed FCS. Prior to the assay, [^{3}H]-adenine was added to the medium (3 μCi/ml) and cells were incubated for 2 h in 5% CO_2 atmosphere at 37 °C. Cells were washed 3× with 1 ml of a medium, constituted by DMEM-F12 and 25 mM HEPES (pH 7.4) and pre-incubated with assay medium containing 30 μM rolipram at 37 °C for 15 min. Compound **16b** was incubated for 15 min at 37 °C. Reaction was stopped by adding ice-cold 300 mM perchloric acid containing [^{14}C]-cAMP and cells were maintained at 4 °C for 30 min. The [^{3}H]-cAMP elicited in each well was isolated by chromatographic methods and [^{14}C]-cAMP content allowed to calculate the yield of this isolation. The potency of the compound was expressed as EC_{50}, that is the concentration that elicited 50% of maximal response.

Acknowledgements

We gratefully thank Almirall Prodesfarma SA (Barcelona-Spain) for promoting and funding the present project, Dr. Bernat Vidal (Almirall Prodesfarma) for the preparation of compound **15b**, CESCA-CEPBA for a mobility grant to AC and Prof. Ferran Sanz (GRIB, UPF, Barcelona) for his helpful comments and suggestions in the preparation of the manuscript.

References

[1] V. Ralvic, G. Burnstock, Pharmacol. Rev. 50 (1998) 413–492.

[2] S. Hess, Expert Opin. Ther. Pat. 11 (2000) 1–29.

[3] B.B. Fredhom, G. Arslan, L. Haldner, G. Kull, G. Schulte, W. Wasserman, Nauyn-Schmied. Arch. Pharmacol. 362 (2000) 364–374.

[4] B.B. Fredhom, A.P. Ijzerman, K.A. Jacobson, K.-N. Klotz, J. Linden, Pharm. Rev. 53 (2001) 527–552.

[5] C.E. Müller, B. Stein, Curr. Pharm. Des. 2 (1996) 501–530.

[6] P.G. Baraldi, P.A. Borea, Trends Pharmacol. Sci. 21 (2000) 456–459.

[7] P.G. Baraldi, B. Cacciari, R. Romagnoli, S. Meringhi, K. Verani, P.A. Borea, G. Spalluto, Med. Res. Rev. 20 (2000) 103–128.

[8] E.M. van der Wenden, A.P. Ijzerman, W.A. Soudijn, J. Med. Chem. 35 (1992) 629–635.

[9] P.G. Baraldi, B. Cacciari, S. Moro, G. Spalluto, G. Pastorin, T. Da Ros, K.-N. Klotz, K. Varani, S. Gessi, P.A. Borea, J. Med. Chem. 45 (2002) 770–780.

[10] W. Soudijn, I. Van Wijngaarden, A.P. Ijzerman, Curr. Top. Med. Chem. 3 (2003) 355–367.

[11] G. Cristalli, C. Lambertucci, S. Taffi, S. Vittori, R. Volpini, Curr. Top. Med. Chem. 3 (2003) 387–401.

[12] C.E. Müller, Curr. Top. Med. Chem. 3 (2003) 445–462.

[13] P.G. Baraldi, M.A. Tabrizi, A. Bovero, B. Avitabile, D. Preti, F. Fruttarolo, R. Romagnoli, K. Varani, P.A. Borea, Eur. J. Med. Chem. 38 (2003) 367–382.

[14] M.P. De Ninno, H. Masamune, L.K. Chenard, K.J. Di Rico, C. Eller, J.B. Etienne, J.E. Tickner, S.P. Kennedy, D.R. Knight, J. Kong, J.J. Oleynek, R. Tracey, R.J. Hill, J. Med. Chem. 46 (2003) 353–355.

[15] R. Volpini, S. Costanzi, S. Vittori, G. Cristalli, K.-N. Klotz, Curr. Top. Med. Chem. 3 (2003) 427–433.

[16] Y.C. Kim, X. Jin, N. Melman, J. Linden, K.A. Jacobson, J. Med. Chem. 43 (2000) 1165–1172.

[17] A.M. Hayallah, J. Sandoval-Ramírez, U. Reith, U. Schobert, B. Preiss, B. Schumacher, J.W. Daly, C.E. Müller, J. Med. Chem. 45 (2002) 1500–1510.

[18] S.-A. Kim, M.A. Marshall, N. Melman, H.S. Kim, C.E. Müller, J. Linden, K.A. Jacobson, J. Med. Chem. 45 (2002) 2131–2138.

[19] P.G. Baraldi, M.A. Tabrizi, D. Preti, A. Bovero, R. Romagnoli, F. Fruttarolo, N.A. Zaid, A.R. Moorman, K. Varani, S. Gessi, S. Merighi, P.A. Borea, J. Med. Chem. 47 (2004) 1434–1447.

[20] A. Rubino, V. Ralevic, G. Burnstock, Br. J. Pharmacol. 115 (1995) 648–652.

[21] H. Harada, O. Osamu Asano, Y. Hoshino, S. Yoshikawa, M. Matsukura, Y. Kabasawa, J. Nijima, Y. Kotake, N. Watanabe, T. Kawata, T. Inoue, T. Horizoe, N. Yasuda, H. Minami, K. Nagata, M. Murakami, J. Nagaoka, S. Kobayashi, I. Tanaka, S. Abe, J. Med. Chem. 44 (2001) 170–179.

[22] M.B. Grant, R.W. Tarnuzzer, S. Caballero, M.J. Ozeck, M.I. Davis, P.E. Spoerri, I. Feoktistov, I. Biaggioni, J.C. Shryock, L. Berladinelli, Circ. Res. 85 (1999) 699–706.

[23] C.E. Müller, Drugs Future 25 (2000) 1043–1052.

[24] J.A. Auchampach, J. Jin, T.C. Wan, G.H. Caughey, J. Linden, Mol. Pharmacol. 52 (1998) 846–860.

[25] G.R. Strohmeier, S.M. Reppert, W.I. Lencer, J.L. Madara, J. Biol. Chem. 270 (1995) 2387–2394.

[26] I. Feostikov, I. Baggioni, Pharmacol. Rev. 49 (1997) 381–402.

[27] K.A. Jacobson, A.P. Ijzerman, J. Linden, Drug Dev. Res. 47 (1999) 45–53.

[28] J.R. Fozard, Curr. Opin. Pharmacol. 3 (2003) 264–269.

[29] A. Maconi, G. Pastorin, T. Da Ros, G. Spalluto, Z.G. Gao, K.A. Jacobson, P.G. Baraldi, K. Varani, S. Moro, P.A. Borea, J. Med. Chem. 45 (2002) 3579–3582.

[30] E. Ongini, A. Monopoli, B. Cacciari, P.G. Baraldi, Farmaco 56 (2001) 87–90.

[31] C.E. Müller, Farmaco 56 (2001) 77–80.

[32] A.S. Robeva, R. Woodward, X. Jin, Z. Gao, S. Bhattacharya, H.E. Taylor, D.L. Rosin, J. Linden, Drug. Dev. Res. 39 (1996) 243–252.

[33] B. Grahner, S. Winiwarter, W. Lanzner, C.E. Müller, J. Med.Chem. 37 (1994) 1526–1534.

[34] The amino derivatives **3b** and **15b** were obtained through the basic hydrolysis of the corresponding 1,3-dimethyl [**4b**] and 1,3-dipropyl (see Ref. [35]) acetamido derivatives, respectively.

[35] A. Stefanachi, F. Leonetti, A. Cappa, A. Carotti, Tetrahedron Lett. 44 (2003) 2121–2123.

[36] Quantum mechanical MEP computation was carried by means of the MIPSIM software [38]. The required *ab initio* wave functions were obtained with the GAMESS program: M.W. Schmidt, K.K. Baldridge, J.A. Boatz, S.T. Elbert, M.S. Gordon, J.H. Jensen, S. Koseki, N. Matsunaga, K.A. Nguyen, S.J. Su, T.L. Windus, M. Dupuis, J.A. Montgomery, J. Comput. Chem. 14 (1993) 1347–1363.

[37] M. Orozco, F.J. Luque, Molecular Electrostatic Potentials: Concepts and Applications. Theoretical and Computational Chemistry, J.S. Murray, K. Sen (Eds.), Elsevier, Amsterdam vol. 3, 1996, pp. 181–218.

[38] M. de Cáceres, J. Villà, J.J. Lozano, F. Sanz, Bioinformatics 16 (2000) 568–569.

[39] ACD, version 7.0, Toronto, Canada.

[40] c-LOGP, version 4.5, Biobyte, Claremont, CA, USA.

[41] Biological data of xanthine derivatives are not shown in this paper; they came from a collaborative study with Prof. Franco Fernandez of the University of Santiago de Compostela (Spain) and are unpublished yet.

[42] The multiple linear regression analysis has been carried out by means of the QSAR module of the molecular modeling software package of Sybyl (version 6.8, Tripos Ass., St. Louis, Missouri).

[43] H. Kubinyi, QSAR: Hansch Analysis and Related Approaches; R. Mannhold, P. Krogsgaard-Larsen, H. Timmerman (Eds.), VCH, Weinheim, New York 1993.

[44] C. Hansch, A. Leo, D. Hoekman, Exploring QSAR Hydrophobic, Electronic, and Steric Constants, vol. 2, ACS Professional Reference Book, American Chemical Society, Washington, DC, 1995.

[45] S. Wold, L. Eriksson, Statistical validation of QSAR results. Chemometrics Methods in Molecular Design, H. Van de Waterbeemd (Ed.), VCH, Weinheim, 1996, pp. 309–318.

[46] R.G. Brenton, Chemometrics, Data Analysis for Laboratory and Chemical Plant, Wiley, England, 2003 15–117.

[47] Y.C. Cheng, W.H. Prusoff, Biochem. Pharmacol. 22 (1973) 3099–3108.

[48] Y. Salomon, Adv Cyclic Nucleotide Res. 10 (1979) 35–55.